University of South Carolina
Scholar Commons

11-14-2014

Self-Assembly and Ring-Opening Metathesis Polymerization of a Bifunctional Carbonate–Stilbene Macrocycle

Yuewen Xu
University of South Carolina - Columbia

Weiwei L. Xu
University of South Carolina - Columbia

Mark D. Smith
University of South Carolina - Columbia, mdsmith3@mailbox.sc.edu

Linda S. Shimizu
University of South Carolina - Columbia, shimizul@mail.chem.sc.edu

Follow this and additional works at: https://scholarcommons.sc.edu/chem_facpub

Part of the Polymer Chemistry Commons

RSC Advances

Self-assembly and ring-opening metathesis polymerization of a bifunctional carbonate–stilbene macrocycle†

Yuewen Xu, Weiwei L. Xu, Mark D. Smith and Linda S. Shimizu*

A carbonate–stilbene bifunctional macrocycle was readily synthesized, and its assembly was studied by crystallization from several solvents. The macrocycle displayed columnar assembly from less polar solvents (THF and CH_2Cl_2), while a more compact structure was observed from 9 : 1 CH_2Cl_2–acetone. All structures displayed organization through the C–H⋯O hydrogen bonding motif as well as through aryl stacking interactions. Upon dissolution and treatment with Grubbs' II catalyst, this 30-membered ring underwent entropy-driven ring-opening metathesis polymerization (ED-ROMP) to give a precisely linear alternating A–B–A–B copolymer. This design of a single macrocyclic building block allows the formation of supramolecular self-assembly in the solid-state while affording a linear alternating polymer from solution.

1 Introduction

Macrocyclic materials have demonstrated utility in natural product synthesis,[1] for porous materials[2,3] and in supramolecular chemistry.[4,5] Our group has developed bis-urea macrocycles as assembly units to form columnar materials with homogeneous and accessible columns that can be used for binding guests and for facilitating reactions in confinement.[6,7] Salient features of this supramolecular assembly unit include relatively unstrained macrocycles that consist of two rigid spacers and two urea groups. The bis-urea macrocycles self-assemble into columns through a three-centered urea hydrogen-bonding motif and aryl stacking interactions. In this manuscript, we investigated the substitution of carbonate groups for the ureas. The thirty membered ring of macrocycle **1** incorporates both stilbene and carbonate moieties (Fig. 1). We evaluated the assembly of these macrocycles under a range of conditions, and found that these macrocycles also self-assembled into columns in the solid-state with the monomers organized through dipole interactions and CH⋯O hydrogen bonds. We evaluated the macrocycle by DFT methods and estimated that they were relatively unstrained, suggesting that a polymerization should not be an enthalpy driven process. Experiments showed that the macrocyclic monomers were polymerized using Grubbs' catalysts second generation and supported the hypothesis that this polymerization was an entropy driven process.

Aromatic polycarbonates are important engineering plastics, especially those manufactured from bisphenol A, which are transparent and have relatively high glass transition temperatures and good processability.[8,9] Aliphatic polycarbonates are attracting attention for medical applications due to their biocompatibility and degradability.[10] Typically, aromatic polycarbonates, such as those derived from bisphenol A, are made from the corresponding phenol and phosgene or its derivatives. Aliphatic derivatives are synthesized by ring-opening polymerization of cyclic carbonates or spiroorthocarbonate monomers using anionic, cationic, coordination–insertion, organocatalytic or enzymatic methods.[11] These cyclic monomers are often strained 3–8 membered rings, and the polymerization is driven by enthalpy that is associated with the release of ring strain.[12] The polymerization of large cyclic carbonates with relatively low ring strain is thought to be entropy driven.[13] Entropy driven ring-opening metathesis (ED-ROMP) is relatively rare,[14–18] and polymers are favoured at high monomer concentrations. Macrocyclic alkenes and esters have been polymerized by entropy driven polymerizations.[12] For example, Hodge and Kamau observed ED-ROMP of macrocyclic

Department of Chemistry and Biochemistry, University of South Carolina, 631 Sumter St, Columbia, SC 29208, United States. E-mail: shimizls@mailbox.sc.edu; Fax: +1 803-777-9521; Tel: +1 803-777-2066
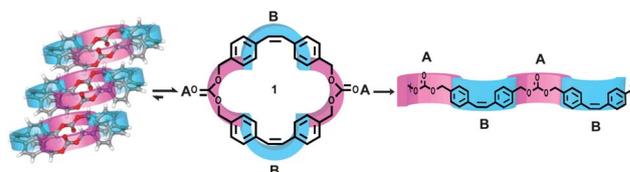
Fig. 1 Bifunctional macrocycle **1** self-assembled to give columnar structures in the solid-state. Upon dissolution and treatment with Grubbs' catalyst, the macrocycle undergoes a ring-opening polymerization.

olefins with 21-, 28-, and 38-membered rings.[19] Gautrat and Zhu reported the ROP of cyclic bile acids (35- and 38-membered rings) to afford degradable elastomers.[20] This manuscript reports the ED-ROMP of a 30-membered dicarbonate macrocycle to give an alternating copolymer.

Copolymers are of great interests to polymer chemists.[21] A block copolymer can introduce phase separation of two blocks and maintain its individual function. Random copolymers allow readily tuning of material properties, such as crystallinity and glass transition temperature, by varying the composition of the two monomers along the polymer backbones. In comparison, precisely alternating copolymers could render optimal positioning of two monomers and introduce extra fine microstructure. Thus, they could be useful in a variety of applications, such as organic light emitting diodes.

Our symmetrical macrocycle is bifunctional and contains both carbonates and stilbenes. Upon ring-opening metathesis polymerization using Grubbs' II catalyst, macrocycle **1** produces a precisely alternating copolymer, where carbonate and stilbene groups were aligned next to each other. We used computations to estimate the ring strain present in **1** and investigated the subsequent ring-opening polymerization of the macrocycle. The polymerization was clearly concentration dependent with lower concentration (0.2 M) affording relatively low yield of polymer while higher concentrations (1 M) showed significant improvement in both yield and molecular weight. We observed significant isomerization of the *cis*-stilbene under our polymerization conditions to give a *trans* : *cis* ratio of ~8 : 5. These new polycarbonates may have interesting material properties and applications.

2   Experimental

2.1   Materials

All chemicals were purchased from Sigma-Aldrich or VWR and used without further purification. HPLC grade chloroform was used for ring-opening metathesis polymerization and was vacuum distilled over CaH$_2$ prior to use.

2.2   Synthesis

Synthesis of *cis*-stilbene diol 3. A solution of LiAlH$_4$ (0.274 g, 6.87 mmol) was prepared in ~30 mL THF and stirred for 30 minutes at 0 °C. Then *cis*-stilbene-4,4′-dicarboxylate **2** (0.925 g, 3.12 mmol) was dissolved in 50 mL THF and transferred to an addition funnel. The dicarboxylate was added dropwise to the LiAlH$_4$ solution and stirred for 6 hours at r.t. The reaction was then quenched with 0.3 mL H$_2$O, 0.6 mL 1 N NaOH, followed by 0.9 mL H$_2$O. After completion, the reaction mixture was filtered and the solution was dried over Na$_2$SO$_4$ anhydrous and reduced *in vacuo*. The product was obtained as a white solid (0.71 g, 95%). Data: mp 116–119 °C. ^{1}H NMR (300 MHz, DMSO-d_6) δ 4.44 (d, J = 6.0 Hz, 4H), 5.15 (t, J = 6.0 Hz, 2H), 6.57 (s, 2H), 7.18 (s, 8H); ^{13}C NMR (75 MHz, DMSO-d_6) δ 63.3, 127.1, 128.9, 130.3, 135.9, 142.3. MS (EI), m/z = 179, 193, 221, 240 (M$^+$); HRMS (EI) calcd for C$_{16}$H$_{16}$O$_2$ 240.1150, found 240.1147.

Synthesis of macrocycle 1. Solid 1,1′-carbonyldiimidazole (0.337 g, 2.08 mmol) was introduced to a solution of *cis*-stilbene

diol **3** (0.50 g, 2.08 mmol) in 50 mL THF.[22] The reaction mixture was stirred at 70 °C for 48 h. The solvent was removed under reduced pressure. Then the residue was subjected column chromatography on silica gel and eluted with CH$_2$Cl$_2$–hexane (3 : 1) to afford a white powder (0.26 g, 41%). Data: ^{1}H NMR (400 MHz, CDCl$_3$) δ 5.16 (s, 8H), 6.62 (s, 4H), 7.18–7.24 (m, 16H); ^{13}C NMR (100 MHz, CDCl$_3$) δ 69.7, 128.1, 129.3, 130.5, 133.8, 137.6, 155.1. MS (EI), m/z = 178, 207, 221, 267, 488, 532 (M$^+$); HRMS (EI) calc. for C$_{34}$H$_{28}$O$_6$ 532.1886, found 532.1891.

2.3   Ring-opening polymerization

The following experiment is typical of those summarized in Table 1: macrocycle **1** (0.145 g) was dissolved CHCl$_3$ (0.2 mL) at a concentration of ~1 M. The solution was degassed by freeze–pump–thaw method and refilled with nitrogen. Grubbs' catalyst 2nd generation in minimum degassed CHCl$_3$ (~0.07 mL) was introduced into the reaction mixture. The reaction mixture was allowed to react at 60 °C for 18 h before quenched with trace amount of ethyl vinyl ether. The solution was allowed to stir at room temperature for another 30 minutes and diluted with 0.5 mL CHCl$_3$. Cold methanol was added to the solution dropwise until a layer of precipitated polymer was found, and the resulting polymer was collected. The precipitation was repeated to remove any unreacted monomer, and then the resulting polymer was dried under vacuum overnight. Data: ^{1}H NMR (500 MHz, CDCl$_3$) δ 5.13 (s), 5.16 (s), 6.58 (s), 7.09 (s), 7.23 (s), 7.37 (d), 7.49 (d); ^{13}C NMR (125 MHz, CDCl$_3$) δ 69.7, 126.9, 128.5, 128.8, 129.0, 129.2, 130.3, 134.1, 134.7, 137.5, 137.6, 155.2.

2.4   X-ray diffraction

Table 1 Crystal and refinement data for crystal forms of **1** obtained from CH$_2$Cl$_2$, THF and 9 : 1 CH$_2$Cl$_2$–acetone

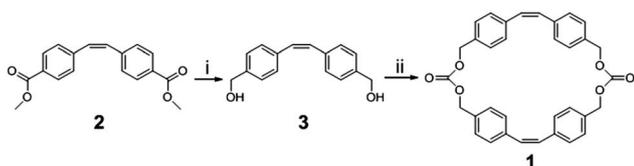|	**1**·CH$_2$Cl$_2$	**1**·C$_4$H$_8$O	**1**
Empirical formula	C$_{35}$H$_{30}$Cl$_2$O$_6$	C$_{38}$ H$_{36}$O$_7$	C$_{34}$H$_{28}$O$_6$
Formula weight	617.49	604.67	532.56
T/K	150(2)	100(2)	150(2)
Crystal system	Triclinic	Monoclinic	Monoclinic
Space group	$P\bar{1}$	$P2_1/n$	$P2_1/c$
a/Å	10.9128(8)	14.555(4)	11.2731(8)
b/Å	11.6446(8)	5.6690(16)	10.6669(7)
c/Å	12.4210(9)	18.310(5)	22.7178(15)
α/°	97.081(1)	90	90
β/°	100.513(1)	96.521(6)	91.852(2)
γ/°	98.806(1)	90.00	90
V/Å^3	1514.93(19)	1501.0(7)	2730.4(3)
Z	2	2	4
D_c/mg mm^{-3}	1.354	1.338	1.296
μ/mm^{-1}	0.260	0.092	0.088
$F(000)$	644	640	1120
Refl. collected, unique	21 031, 5346	16 358, 3122	30 839, 4848
R_{int}	0.0433	0.0517	0.0662
GOF on F^2	1.065	1.022	0.912
$R_1[I > 2\sigma(I)]$	0.0492	0.0416	0.0394
wR_2 (all data)	0.1449	0.1011	0.0840
$\Delta\rho_{max,min}$/e Å^{-3}	0.588/−0.458	0.24/−0.21	0.387/−0.128

2.5 Characterization

NMR was recorded on Varian Mercury/VX 300 and 500 NMR spectrometer. Size-exclusion chromatography (SEC) was conducted on a liquid chromatograph (Agilent 1100 series) equipped with an HP1047A refractive index detector. Molecular weight characteristics of the samples were referenced to polystyrene standards (Polymer Laboratories). DSC data were collected on a TA Q200 differential scanning calorimeter. X-ray diffraction data were collected on Bruker SMART APEX diffractometer using Mo Kα radiation. The powder X-ray diffraction experiments were performed on Rigaku D/Max 2100 Powder X-ray diffractometer (Cu Kα radiation), and the experiments were taken using a zero background slide on which the sample was gently pressed. The N_2 gas adsorption isotherm was generated by using Micromeritics ASAP 2020 instrument. UV-vis detection was performed on a Beckman Coutler 640 DU spectrometer.

3 Results and discussion

The cis-stilbene diol **3** was synthesized from commercial dimethyl cis-stilbene-4,4′-dicarboxylate **2** as described previously.[23] The diol was then cyclized with 1,1′-carbonyldiimidazole in THF (40 mM) under refluxing condition to achieve the macrocycle **1** in a moderate yield (Scheme 1). No extra base was required, since the nitrogen on imidazole ring was sufficiently basic. The dimeric and symmetrical structure of **1** was confirmed by NMR and Mass spectrometry. X-ray quality single crystals of **1** were obtained by slow evaporation of CH_2Cl_2 (2 mg mL^{-1}) to afford transparent plate-like crystals of the solvate $C_{34}H_{28}O_6 \cdot CH_2Cl_2$, from THF (2 mg mL^{-1}) to give colorless needle crystals of the THF solvate $C_{34}H_{28}O_6 \cdot C_4H_8O$, and a solvent free crystal obtained by slow evaporation from 9 : 1 CH_2Cl_2–acetone (2 mg mL^{-1}). Table 1 compares their crystal data. In the case of the solvate structures, each formed supramolecular columnar structures in which one solvent molecule filled the cavity of the macrocyclic monomer.

Macrocycle **1** crystallized from CH_2Cl_2 in the triclinic system with space group $P\bar{1}$. The asymmetric unit consists of one $C_{34}H_{28}O_6$ molecule and one encapsulated CH_2Cl_2 molecule (Fig. 2a and b). Unexpectedly, the carbonate macrocycle assembled into columns assisted by four short C–H⋯O interactions.[24,25] Blue lines in Fig. 2b indicate interactions with distances at least 0.2 Å shorter than the sum of the van der Waals radii of H and O (2.72 Å). Donor–acceptor (D(H)–A) distances range from 3.278(2) for C2(H2A)⋯O5′ to 3.467(2) for C17(H17B)⋯O1′. Dichloromethane molecules were encapsulated within the columnar host structures through contacts

Fig. 2 Views from the crystal structure of **1**·CH_2Cl_2 solvate. (a) Molecular structure of the macrocycle. Displacement ellipsoids drawn at the 50% probability level; (b) a tubular array organized by C–H⋯O hydrogen bonds, indicated by blue lines; (c) packing diagram looking down the column axis. CH_2Cl_2 solvent molecules fill the columns.

between the hydrogens of CH_2Cl_2 and the carbonate oxygen that give short donor–acceptor (D(H)–A) distances of (C(H)⋯OCO_2 = 3.62 Å) as well as to the neighboring aryl group (H⋯centroid 3.18 Å).

Columnar assembly was also observed in the THF solvate $C_{34}H_{28}O_6 \cdot C_4H_8O$. The compound crystallized as colorless needles in the monoclinic space group $P2_1/n$. The asymmetric unit consists of half of one macrocycle, which is located on a crystallographic inversion center, and a THF molecule (Fig. 3). The THF is disordered across the inversion center. The macrocycles stack into columns through CH⋯O interactions between the methylenes of **1** and the carbonyl oxygen of a neighboring macrocycle with a D⋯A distance of 3.492(2) from C(17)⋯O(1). Fig. 3b displays these short CH⋯O contacts as well as those between

Scheme 1 Synthesis of macrocycle **1**. Reagents and conditions: (i) $LiAlH_4$, THF, 95%; (ii) 1,1′-carbonyldiimidazole, THF, reflux, 41%.

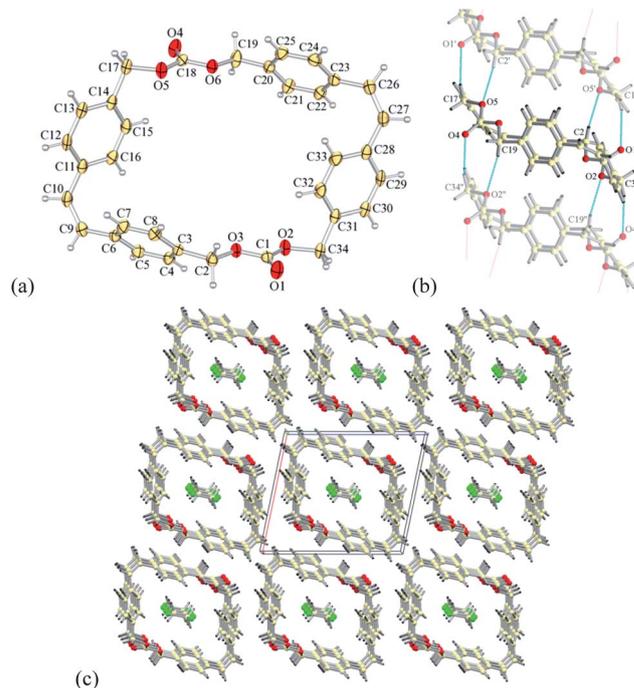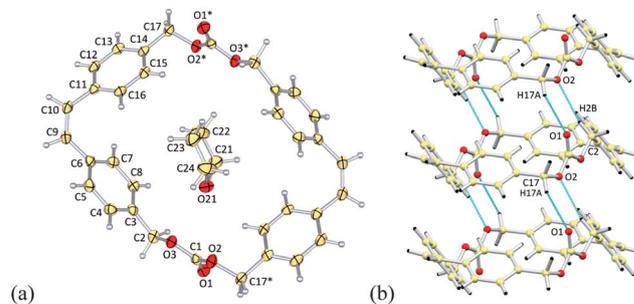Fig. 3 Views from the crystal structure of **1**·THF solvate. (a) Molecular structure with inclusion of THF in the macrocycle; (b) a tubular array viewed from the side. Blue lines represent C–H⋯O hydrogen bonds.

carbonate ester oxygen O2 and methylene adjacent to carbonate (H2) with D⋯A = 3.548(2) Å from C(2)⋯O(2). The cycles make an angle of 58.67(1)° with the column axis. The column is filled with THF solvates likely in contact with the column walls through CH⋯O and van der Waals interactions, though such analysis is less reliable because of the THF disorder.

A different, solvent-free crystal form was obtained by crystallization from 9 : 1 CH_2Cl_2–acetone. The colorless block crystals are monoclinic with the space group $P2_1/c$. The macrocycles assemble primarily through CH–O interactions. Fig. 4b shows the short CH⋯O interactions between the carbonate oxygen (O4) and C–H donors on two neighboring macrocycles. The donor–acceptor (D(H)–A) distances are 3.250(2) Å from C(10) to O(4) and 3.247(2) Å from C34 to O4. In addition, we observed offset face-to-face stacking interactions (illustrated by pairs of like color) and edge-to-face (two molecules of unlike color) stacking interactions (Fig. 4c).

It appears that CH⋯O short contacts are an important organizational element in each of the three crystal forms. The small, low polarity solvents CH_2Cl_2 and THF were included in the channels of these columns. The self-assembly of macrocycles by non-covalent interactions has also been used to generate confined environments that can influence organic reactions.[26] Thus, we were interested to see if the columnar structures would be porous after the solvent was evacuated.

Removal of the dichloromethane under vacuum (48 h) caused a marked change in the morphology of the crystals, experimentally suggesting that the interactions that hold the carbonate macrocycles together are not as robust as the urea interactions that typically drive our bis-urea macrocycles into stable columnar structures.[6,7] We next investigated the porosity of these crystals. Crystals of **1** (145 mg) obtained from CH_2Cl_2 after vacuum drying were subjected to N_2 gas adsorption measurement at 77 K. We observed a type II isotherm (Fig. 5a), which is consistent with mesoporous materials.[27] The BET method was applied to the isotherm at P/P_o between 0.06 and 0.2 to give a calculated surface area of 314 m^2 g^{-1}. The pore volume and pore size were calculated as 0.23 cm^3 g^{-1} and 3.32 nm respectively. The results of gas adsorption experiment indicate that, upon removal of the solvent, **1** is mesoporous and shows a pore size that is much larger than the cavity of a single macrocycle.

We turned to powder X-ray diffraction (PXRD) to compare the structure of the desolvated sample with two crystal forms of **1** (**1**·CH_2Cl_2 and the compact structure of **1** from 9 : 1 CH_2Cl_2–acetone). The single crystal data from the crystal forms of **1** were used to generate simulated PXRD patterns using Mercury.[28] Part of the desolvated sample (50 mg) was ground to a powder and examined by PXRD (Fig. 5b, blue line). The pattern is sharp and intense, indicating a highly ordered structure. Comparison of peak positions and intensities of the observed pattern with the two simulated patterns suggests that this structure is distinct from the other crystal forms.

Ring-opening metathesis polymerization (ROMP) is a powerful technique for synthesizing high molecular weight functional polymers.[29] Typically, this type of polymerization takes place in small strained cycle with a size of 3–8 membered ring. The main driving force of polymerization is the release of ring strain, an enthalpically driven process. Larger macrocycles with low ring strain have minimal enthalpy change on polymerization and have less of an enthalpic driving force.[18,30] Monomers with ring strain energy below a critical value of 5 kcal mol^{-1} should not readily polymerize under typical conditions.[13] Thus, we next investigated the ring strain in macrocycle **1**.
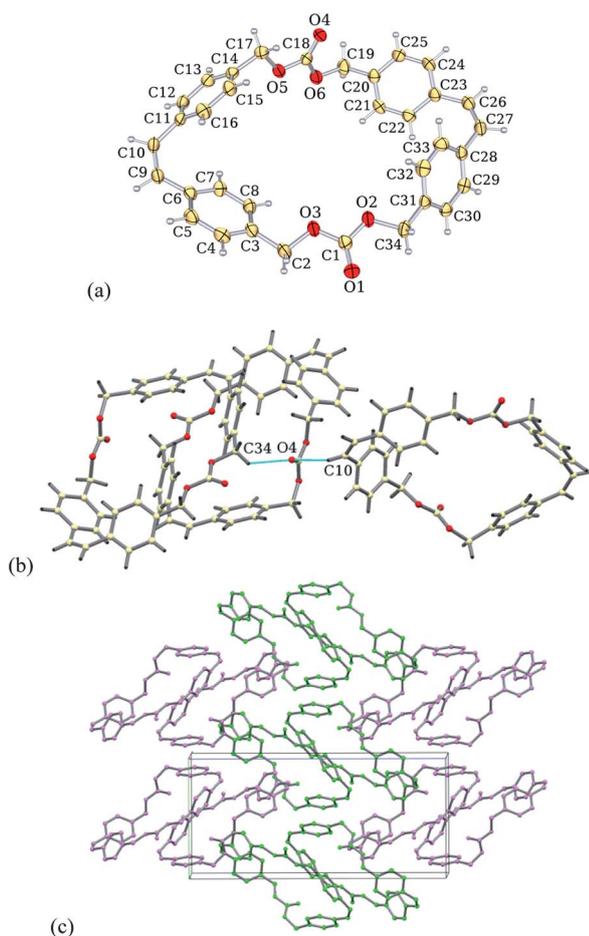

Fig. 4 Views from the crystal structure of **1** obtained from 9 : 1 CH_2Cl_2–acetone. (a) Molecular Structure. (b) View highlighting the short CH⋯O interactions. Blue lines represent C–H⋯O hydrogen bonds; (c) packing diagram of macrocycle **1**. Pairs of like color indicate a face-to-face stacking and pairs of unlike color indicate an edge-to-face stacking.
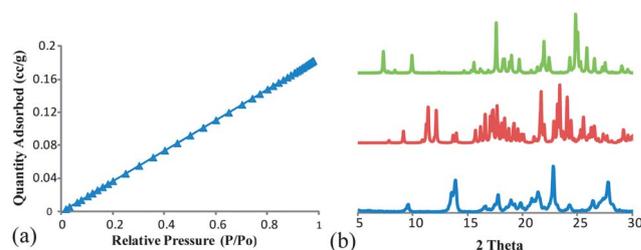

Fig. 5 (a) N_2 gas adsorption isotherm of at 77 K of assembled macrocycle **1**. (b) Experimental PXRD pattern of macrocycle **1** crystal upon solvent removed (blue line), simulated PXRD pattern calculated from the coordinates of **1** (red line), and simulated PXRD pattern calculated from the coordinates of **1**·CH_2Cl_2 single crystal (green line).

Using the crystallographic coordinates (.cif file), we generated a model of macrocycle **1** using *Spartan 10* and deleted the coordinates of CH₂Cl₂ guest.[31] The Monte Carlo search at ground state with Molecular Mechanics (MMFF) force field was carried out to investigate the lowest energy conformer of macrocycle **1**, and the simulated annealing method was used by the program to examine 100 000 conformers and the lowest 100 conformers were kept. We further examined the lowest energy conformer (Fig. 6) by the density functional calculation (DFT) at B3LYP level and using the 6-31+G* basis set, which afford an energy E_1 of -1763.89456 a.u.

To investigate the geometry optimized model in Fig. 6, the C2–C3 and C19–C20 bonds were broken to obtain two identical open chains (fragment **5**). Monte Carlo search was performed to study the conformer distributions of fragment **5**, which has two hydrogens added to the ends of the fragment. A corresponding DFT energy calculation of the lowest energy conformer of fragment **5** was carried out using identical basis set and afforded an energy E_5 of -883.146979 a.u. Because this energy also reflects the formation of two C–H bonds ($E_{C2'-H}$ and $E_{C3'-H}$) and the breaking of C–C bonds (E_{C-C}) as well as any ring strain inherent in **1**. Thus, the ring strain energy E_{RS} of macrocycle **1** should be given by following equation:

$$E_{RS} = E_1 - 2E_5 + 2\Delta E \qquad (1)$$

where

$$\Delta E = E_{C2'-H} + E_{C3'-H} - E_{C-C}. \qquad (2)$$

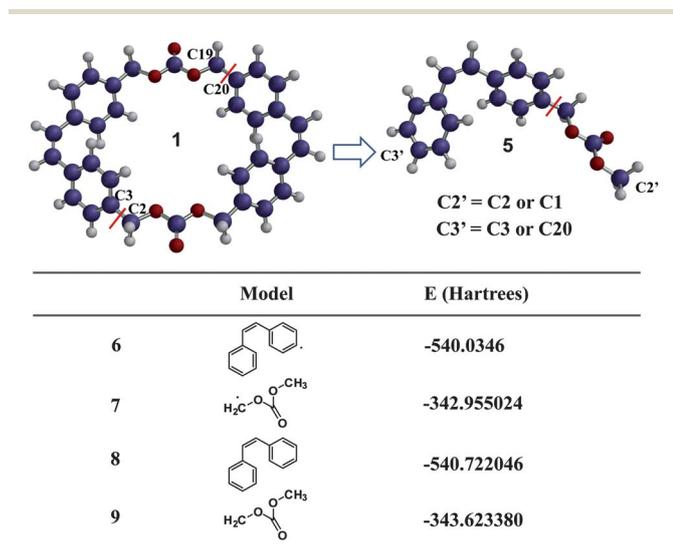| Model		E (Hartrees)
6		−540.0346
7		−342.955024
8		−540.722046
9		−343.623380

Fig. 6 Molecular models simulated by Spartan: geometry optimized model of macrocycle **1** was broken at C2–C3 and C19–C20 bonds to obtain fragment **5**. In order to investigate C–C energy, **5** was divided into radical **6** and **7**; similarly model **8** and **9** were generated to calculate C–H bond energy. All the models were generated by *Spartan 10*, the Monte Carlo search was run at ground state with Molecular Mechanics Force Field (MMFF), energy calculations were processed by the density functional calculation (DFT) at B3LYP level with 6-31+G* basis set.

We estimated the C–C bond energy by breaking the fragment **5** into radical **6** and **7** and calculated the energy of these two radicals by DFT at B3LYP level with 6-31+G* basis set. The C–C bond energy ($E_{C-C} = -0.157355$ a.u.) was determined to the energy difference between fragment **5** and E_6, E_7 of the corresponding radicals. Similarly, models **8** and **9** were designed to estimate the energy of two C–H bonds ($E_{C2'-H}$ and $E_{C3'-H}$) which formed at C2′ and C3′ of fragment **5**, the bond energy was obtained as a difference between the energy of model **8** or **9** and the energy of corresponding radicals, which gives $E_{C2'-H}$ of -0.668356 a.u. and $E_{C3'-H}$ of -0.687446 a.u. Taken together, $\Delta E(-1.198447$ a.u.) was calculated based on eqn (2). This afforded a strain energy E_{RS} of macrocycle **1** of 1.57 kcal mol⁻¹, suggesting relatively little strain. Given this low strain, we were not expecting to observe a ROP under typical conditions.
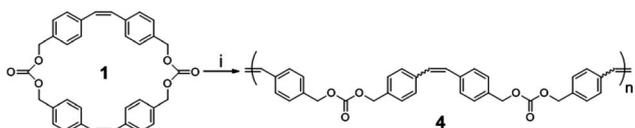
The ring-opening metathesis polymerization of macrocycle **1** was carried out using the highly efficient Grubbs' catalyst second generation and afforded reasonable high-molecular-weight polymers after quenching with ethyl vinyl ether.[32] The polymer was precipitated by addition of methanol. The NMR spectrum of crude reaction mixture upon quenching indicated unreacted monomer and resulting polymer were observed as two major components, although minor fractions of cyclic oligomers were also possible but were not observed from NMR and SEC data. This suggests the cyclic oligomers concentration is very low, <5%.[30] A range of reaction conditions was carried out to investigate the influences of monomer concentration and reaction time on polymerizations. In all cases, the monomer to catalyst ratios were set to 100 : 1 for consistency; therefore, the highest degree of polymerization the polymer could possibly possess would be 100. The polymerization was clearly concentration dependent, since at a lower concentration of 0.2 M the polymerization produced polymer at relatively low yield and molecular weight.[13] However, when the concentration increased to 1 M, which was the highest concentration before monomer started to crystallize from chloroform, the polymerization evidently showed significant improvement in both yield (60%) and molecular weight (M_n = 45 kg mol⁻¹, entry 3 Table 2).[20] Given the polymerization is clearly concentration dependent and that DFT calculations suggest low ring strain, our hypothesis is that the polymerization may be entropy driven. Indeed, Fogg *et al.* suggest that an entropy driving force can be created at appropriately high concentration of cyclic olefins.[33] When ROMP was carried out at a shorter reaction time, we observed similar conversion and molecular weight, which suggests that the reaction equilibrium is likely established within a short period of time.

The ROP affords a copolymer with precise alternation of stilbene and carbonate groups along the macrocycle as illustrated in Scheme 2. The structure of resulting alternating polymer was confirmed from ¹H NMR spectroscopy, which showed a clear distinction from the macrocycle monomer. The *cis*-stilbene is known to isomerize to the more stable *trans*-stilbene under UV-irradiation or thermal initiation.[34–37] In ROMP, *cis* double bond is also known to undergo isomerization to reach toward an equilibration of backbone stereochemistry

Table 2 Summary of ROMP conditions tested

Entry	M/G2[a]	Conc.	t (h)	Conv. (%)	$M_n{}^b$ (kg mol^{-1})	$M_w{}^b$ (kg mol^{-1})	$Đ^b$	$D_p{}^c$
1	~100	0.2 M	18	31	13	20	1.5	24
2	~100	0.7 M	18	55	38	68	1.8	71
3	~100	1 M	18	60	45	86	1.9	85
4	~100	1 M	6	58	43	87	2.0	81

[a] [Monomer] : [catalyst] ratio. [b] Measured using an RI detector on a SEC instrument with chloroform as an eluent at 25 °C. [c] Degree of polymerization.

Scheme 2 Ring-opening metathesis polymerization of macrocycle **1**. (i) **G2**, CHCl₃, 60 °C.

through secondary metathesis.[19,38] The chemical shift of the methylene units of the stilbene are typically used to differentiate between the two isomers.[39] The chemical shift at 7.1 and 6.6 ppm correspond to the vinylic protons (Ha in Fig. 7) on *trans*- and *cis*-stilbene, respectively and are baseline separated in our spectra. Thus, integration of these two gave a *trans* : *cis* ratio of 8 : 5 for entry # 3. This ratio was also observed for the methylene units on *trans*- and *cis*-stilbene (Hb, Fig. 7). Other conditions gave similar ratios. Thus, we observe significant isomerization of the *cis*-stilbene under our polymerization conditions.

The molar mass of resulting polymer was analysed by size exclusion chromatography (SEC). The polymer **4** (entry 3 Table 2) displayed a single peak with a maximum retention time of 20.8 min as shown in Fig. 8a. The polydispersity of polymer **4**

all fell in the range of 1.5–2.0, which is typically observed in the ROMP derived from monomers with a low ring strain.[40–42] Furthermore, the secondary metathesis at extended reaction time (≥6 h) could also contribute to the slight broadening of the molecular weight dispersity.[43,44] The polymer also displayed a single glass transition temperature (T_g) at 73 °C as analysed from differential scanning calorimetry (Fig. 8b) suggesting no microphase separation takes place.

UV-vis spectroscopy provides a further insight into the extended conjugation length of stilbene functionality upon polymerization. The absorption maxima of the solution of macrocycle **1** (2.5×10^{-5} M) originally was displayed at 284 nm, and shifted to a longer wavelength upon polymerization as shown in Fig. 8c. Two major absorption bands at 302 and 316 nm correspond to the *cis* and *trans* stilbene units, respectively and provide additional evidence that isomerization occurs under the reaction conditions. Indeed, the parent *trans*-stilbene should show a $\pi \rightarrow \pi^*$ transition at a higher wavelength due to enhanced conjugation resulting from a more planar geometry of *trans*-stilbene.[45,46]
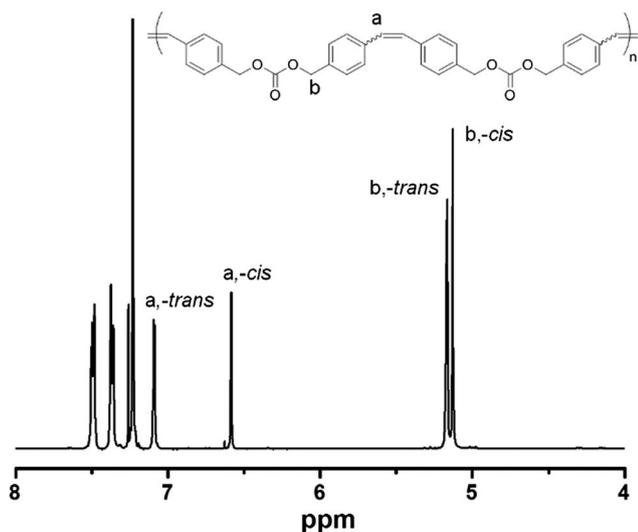

Fig. 7 ¹H NMR spectrum of poly(carbonate-*co*-stilbene) **4** in CDCl₃, 500 MHz.
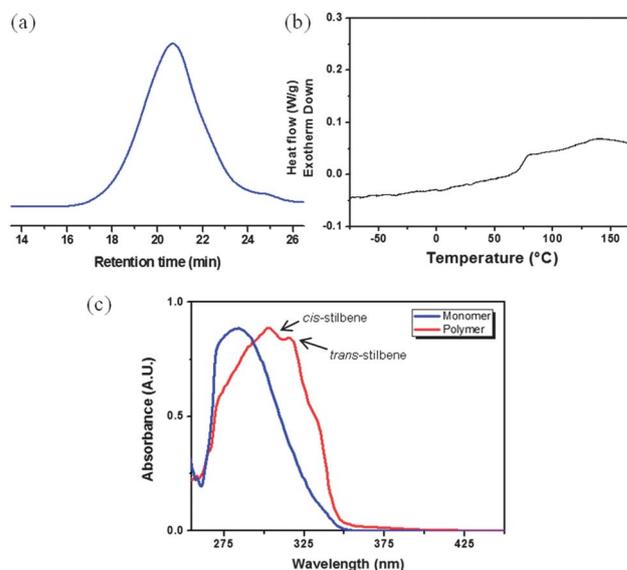

Fig. 8 (a) SEC chromatogram of isolated polymer **4**. Chloroform as eluent at 25 °C. (b) DSC plot of polymer **4** (second heating, 10 °C min⁻¹). (c) Comparison of UV-vis spectra of macrocycle **1** and polymer **4** in chloroform (~2 mg mL⁻¹).

4 Conclusions

The unique design of the stilbene–carbonate macrocycle allowed us to employ this macrocycle as a porous supramolecular self-assembled material in the solid state, as well as a precursor for achieving high molecular-weight precisely alternating polymer. Both carbonate and stilbene units are crucial in that the carbonate moiety provides dipole and hydrogen bonding acceptor capabilities and the stilbene functionality renders cyclic olefin building block necessary for the ring-opening metathesis polymerization. The morphology of solid state assembly was not particularly affected by the solvents tested and displayed columnar structures both from CH_2Cl_2 and THF. The macrocycle successfully underwent ED-ROMP to give a poly(carbonate-*co*-stilbene) copolymer in an alternating manner. Such strategy bridges supramolecular chemistry and traditional polymerization with a single molecular design. We are currently studying the materials properties and degradation rates of these polycarbonates under environmental conditions and hope to report on these shortly.

Acknowledgements

Notes and references

1 X. Xu and D. Sun, *Molecules*, 2013, **18**, 6280.
2 J. An, R. P. Fiorella, S. J. Geib and N. L. Rosi, *J. Am. Chem. Soc.*, 2009, **131**, 8401.
3 K. J. Kilpin, M. L. Gower, S. G. Telfer, G. B. Jameson and J. D. Crowley, *Inorg. Chem.*, 2011, **50**, 1123.
4 R. Chapman, M. Danial, M. L. Koh, K. A. Jolliffe and S. Perrier, *Chem. Soc. Rev.*, 2012, **41**, 6023.
5 W. Zhang and J. S. Moore, *Angew. Chem., Int. Ed.*, 2006, **45**, 4416.
6 L. S. Shimizu, A. D. Hughes, M. D. Smith, M. J. Davie, B. P. Zhang, H.-C. zur Loye and K. D. Shimizu, *J. Am. Chem. Soc.*, 2003, **125**, 14972.
7 M. B. Dewal, Y. Xu, J. Yang, F. Mohammed, M. D. Smith and L. S. Shimizu, *Chem. Commun.*, 2008, 3909.
8 H. T. Pham, S. Munjal and C. P. Bosnyak, in *Handbook of Thermoplastics*, ed. O. Olagoke, Marcel Dekker, New York, pp. 609–640, 1997.
9 H. H. Schobert and C. Song, *Fuel*, 2002, **81**, 15.
10 J. Feng, R.-X. Zhuo and X.-Z. Zheng, *Prog. Polym. Sci.*, 2012, **37**, 211.
11 G. Rokicki, *Prog. Polym. Sci.*, 2000, **25**, 259.
12 S. Strandman, J. E. Gautrot and X. X. Zhu, *Polym. Chem.*, 2011, **2**, 791.
13 K. J. Ivin and J. C. Mol, *Olefin Metathesis and Metathesis Polymerization*, Academic Press, London, 1997.
14 M. J. Marsella, H. D. Maynard and R. H. Grubb, *Angew. Chem., Int. Ed. Engl.*, 1997, **36**, 1101.
15 W. Ast, G. Rheinwalk and R. Kerber, *Makromol. Chem.*, 1976, **177**, 1341.
16 H. Hocker, W. Reimann, L. Reif and K. Riebel, *J. Mol. Catal.*, 1980, **8**, 191.
17 E. A. Ofstead and N. Calderon, *Makromol. Chem.*, 1972, **154**, 21.
18 S. Kang, B. M. Berkshire, Z. Xue, M. Gupta, C. Layode, P. A. May and M. F. Mayer, *J. Am. Chem. Soc.*, 2008, **130**, 15246.
19 P. Hodge and S. D. Kamau, *Angew. Chem., Int. Ed.*, 2003, **42**, 2412.
20 J. E. Gautrot and X. X. Zhu, *Angew. Chem., Int. Ed.*, 2006, **45**, 6872.
21 G. Seipke, H. A. Arfmann and K. G. Wagner, *Biopolymers*, 1974, **13**, 1621.
22 S. P. Rannard and N. J. Davis, *Org. Lett.*, 1999, **1**, 933.
23 Y. Xu, M. D. Smith, J. A. Krause and L. S. Shimizu, *J. Org. Chem.*, 2009, **74**, 4874.
24 O. Takahashi, K. Yamasaki, Y. Kohno, K. Ueda, H. Suezawa and M. Nishio, *Carbohydr. Res.*, 2009, **10**, 1225.
25 K. Shin-ya, O. Takahashi, Y. Katsumoto and K. Ohno, *J. Mol. Struct.*, 2007, **1–3**, 155.
26 J. Yang, M. B. Dewal and L. S. Shimizu, *J. Am. Chem. Soc.*, 2006, **128**, 8122.
27 S. Schlienger, J. Alauzun, F. Michaux, L. Vidal, J. Parmentier, C. Gervais, F. Babonneau, S. Bernard, P. Miele and J. B. Parra, *Chem. Mater.*, 2012, **24**, 88.
28 C. F. Macrae, I. J. Bruno, J. A. Chisholm, P. R. Edgington, P. McCabe, E. Pidcock, L. Rodriguez-Monge, R. Taylor, J. van de Streek and P. A. Wood, *J. Appl. Crystallogr.*, 2008, **41**, 466.
29 G. Black, D. Maher and W. Risse, Living Ring-Opening Olefin Metathesis Polymerization, in *Handbook of Metathesis*, ed. R. H. Grubbs, Wiley-VCH, Weinheim, 2003, vol. 3, pp. 2–71.
30 P. Hodge, Z. Yang, A. Ben-Haida and C. S. McGrail, *J. Mater. Chem.*, 2000, **10**, 1533.
31 *Spartan 10 for Windows, Macintosh and Linux, 1.1.0*, Wavefunction, Inc, Irvine, CA, 2011.
32 A. Michrowska, R. Bujok, S. Harutyunyan, V. Sashuk, G. Dolgonos and K. Grela, *J. Am. Chem. Soc.*, 2004, **126**, 9318.
33 S. Monfette and D. E. Fogg, *Chem. Rev.*, 2009, **109**, 3783.
34 J. Saltiel, E. D. Megarity and K. G. Kneipp, *J. Am. Chem. Soc.*, 1966, **88**, 2336.
35 J. Saltiel, *J. Am. Chem. Soc.*, 1968, **90**, 6394.
36 D. H. Waldeck, *Chem. Rev.*, 1991, **91**, 415.
37 I. Anger, K. Sandros, M. Sundahl and O. Wennerström, *J. Phys. Chem.*, 1993, **97**, 1920.
38 V. Amir-Ebrahimi, D. Byrne, J. G. Hamilton and J. J. Rooney, *Macromol. Chem. Phys.*, 1995, **196**, 327.
39 R. Adhikary, C. A. Barnes, R. L. Trampel, S. J. Wallace, T. W. Kee and J. W. Petrich, *J. Phys. Chem. B*, 2011, **115**, 10707.
40 A. Demonceau, A. W. Stumpf, E. Saive and A. F. Noels, *Macromolecules*, 1997, **30**, 3127.

41 D. M. Lynn, S. Kanaoka and R. H. Grubbs, *J. Am. Chem. Soc.*, 1996, **118**, 784.

42 A. W. Stumpf, E. Saive, A. Demonceau and A. F. Noels, *J. Chem. Soc., Chem. Commun.*, 1995, 1127.

43 C. W. Bielawski and R. H. Grubbs, *Prog. Polym. Sci.*, 2007, **32**, 1.

44 M. A. Hillmyer and R. H. Grubbs, *Macromolecules*, 1995, **28**, 8662.

45 J. G. Graselli and W. M. Ritchey, *Atlas of Spectral Data and Physical Constants*, 1975, p. 399.

46 A. Coleman, S. M. Draper, C. Long and M. T. Pryce, *Organometallics*, 2007, **26**, 4128.